Injectable hydrogel properties influence infarct expansion and extent of postinfarction left ventricular remodeling in an ovine model

Jamie L. Ifkovits[a], Elena Tous[a], Masahito Minakawa[b,c], Masato Morita[b,c], J. Daniel Robb[b,c], Kevin J. Koomalsingh[b,c], Joseph H. Gorman III[b,c], Robert C. Gorman[b,c], and Jason A. Burdick[a,1]

[a]Department of Bioengineering, University of Pennsylvania, Philadelphia, PA 19104; [b]Gorman Cardiovascular Research Group, University of Pennsylvania, Glenolden, PA 19036; and [c]Department of Surgery, University of Pennsylvania, Philadelphia, PA 19104

Edited by Robert Langer, Massachusetts Institute of Technology, Cambridge, MA, and approved May 19, 2010 (received for review March 29, 2010)

A recent trend has emerged that involves myocardial injection of biomaterials, containing cells or acellular, following myocardial infarction (MI) to influence the remodeling response through both biological and mechanical effects. Despite the number of different materials injected in these approaches, there has been little investigation into the importance of material properties on therapeutic outcomes. This work focuses on the investigation of injectable hyaluronic acid (MeHA) hydrogels that have tunable mechanics and gelation behavior. Specifically, two MeHA formulations that exhibit similar degradation and tissue distribution upon injection but have differential moduli (~8 versus ~43 kPa) were injected into a clinically relevant ovine MI model to evaluate the associated salutary effect of intramyocardial hydrogel injection on the remodeling response based on hydrogel mechanics. Treatment with both hydrogels significantly increased the wall thickness in the apex and basilar infarct regions compared with the control infarct. However, only the higher-modulus (MeHA High) treatment group had a statistically smaller infarct area compared with the control infarct group. Moreover, reductions in normalized end-diastolic and end-systolic volumes were observed for the MeHA High group. This group also tended to have better functional outcomes (cardiac output and ejection fraction) than the low-modulus (MeHA Low) and control infarct groups. This study provides fundamental information that can be used in the rational design of therapeutic materials for treatment of MI.

infarction | cardiac | mechanics | polymer | biomaterial

Left ventricular (LV) remodeling caused by a myocardial infarction (MI) is responsible for almost 70% of the 5 million cases of heart failure that have occurred in the United States in recent years (1). Early infarct expansion or stretching has been associated with poor long-term prognosis (2–4) and has been identified as the mechanical phenomenon that initiates and sustains the process of adverse post-MI LV remodeling that leads to heart failure (5–10). Infarct expansion causes abnormal stress distribution in myocardial regions outside the infarction, especially in the adjacent borderzone region, putting this region at a mechanical disadvantage. With time, increased regional stress is the impetus for several maladaptive biologic processes, such as myocyte apoptosis and matrix metalloproteinase activation, that inherently alter the contractile properties of normally perfused myocardium (11, 12). Once initiated, these maladaptive processes lead to a heart failure phenotype that is difficult to reverse by medical or surgical means.

We have demonstrated that ventricular restraint early after MI reduces infarct expansion and limits long-term global LV remodeling in large-animal infarction models (10, 13–16). To circumvent the surgical placement of restraining devices early post-MI, our group and others have begun to explore the use of injectable materials to limit infarct expansion and normalize the regional stress distribution (17–26). Such an approach offers the potential for a noninvasive, catheter-based treatment that could be administered early post-MI to attenuate the remodeling process and prevent the development of heart failure. Despite the range of material types and properties that have been injected, no studies have systematically investigated the effect of material properties (e.g., mechanics) on structural and functional outcomes. Such information will be extremely important in developing the optimal material for preventing infarct expansion and the associated remodeling.

This study focuses on the assessment of injectable modified hyaluronic acid hydrogels to stiffen/thicken the infarct area to limit the associated borderzone expansion, limit LV dilation, and improve global function in an established, clinically relevant ovine infarction model. Specifically, to eliminate mass loss and tissue distribution as variables, injectable formulations of hyaluronic acid hydrogels were designed that have similar degradation and gelation behavior but have varied mechanical properties.

Results

Hydrogel Mechanics Are Dependent on the Extent of Modification and Initiator Parameters. Two methacrylated hyaluronic acid macromers (MeHA) with varying amounts of methacrylate substitution were synthesized. The extent of modification was found to be ~30% (MeHA Low) or ~60% (MeHA High) by ^{1}H NMR. Hydrogels were prepared from the macromers (maintained at 4% by weight) upon combination with the bicomponent redox initiation system of ammonium persulfate (APS) and N,N,N′,N′-tetramethylethylenediamine (TEMED) (Fig. S1). Rheometry was used to monitor the storage (G', defined as the fourth consecutive point with <1% change) and loss modulus (G'') of hydrogels formed from the different macromer and initiator combinations (Fig S2 for a representative time sweep curve). A significant difference between the G' of the two hydrogels formed with identical initiator concentrations was observed, as was a significant difference between hydrogels formed from the same macromer but different initiator concentrations (Fig. 1*A*). As expected, the time for gelation onset (i.e., G'>G'') decreased as the initiator concentration increased and ranged from ~2.5–4.5 min (Fig. 1*B*). Importantly, the time for gelation was not dependent on the MeHA formulation (i.e., MeHA High versus MeHA Low).

The delivery and penetration of the hydrogel (with dye for visualization) was evaluated by injecting the hydrogel into the apical region of explanted ovine LV tissue. A greater distribution

Author contributions: J.L.I., J.H.G., R.C.G., and J.A.B. designed research; J.L.I., E.T., M. Minakawa, M. Morita, J.D.R., and K.J.K. performed research; J.L.I., E.T., J.D.R., K.J.K., R.C.G., and J.A.B. analyzed data; and J.L.I., R.C.G., and J.A.B. wrote the paper.

The authors declare no conflict of interest.

This article is a PNAS Direct Submission.

[1]To whom correspondence should be addressed. E-mail: burdick2@seas.upenn.edu.

This article contains supporting information online at www.pnas.org/lookup/suppl/doi:10.1073/pnas.1004097107/-/DCSupplemental.

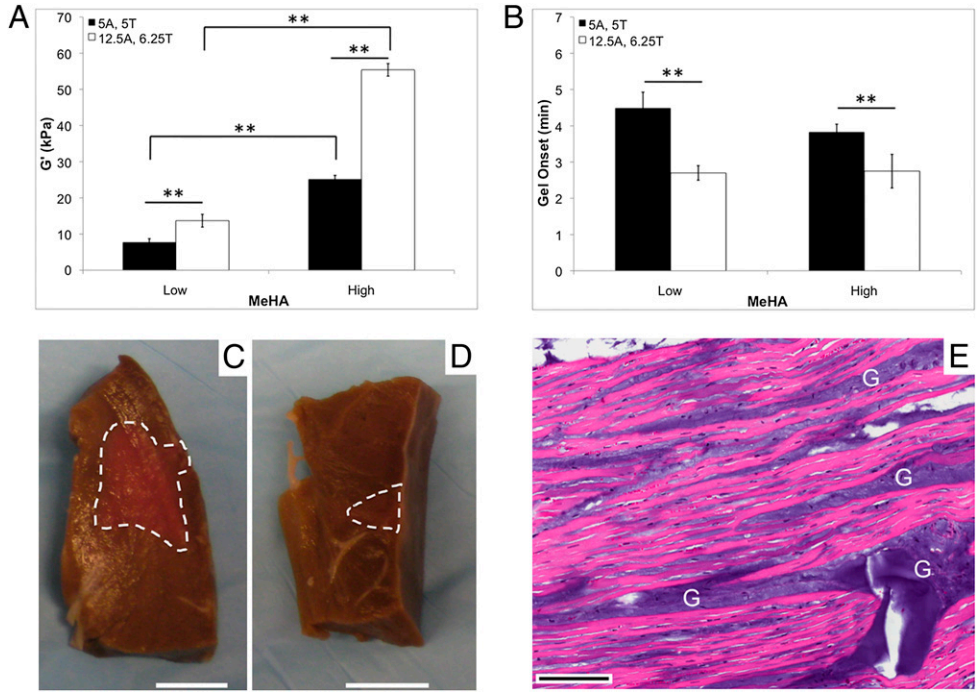

Fig. 1. Hydrogel mechanical properties and gelation time behavior. (*A*) Storage modulus and (*B*) gelation onset time for various macromer (MeHA Low or High) and initiator [5.0 mM/5.0 mM or 12.5 mM/6.25 mM APS (A)/TEMED (T)] combinations. $n = 3$ per group. Data are presented as mean ± SD. $^{**}P < 0.01$. (*C* and *D*) Explanted tissue with 4% by weight MeHA High (outlined with dashed line) gelled with (*C*) 5.0 mM APS/5.0 mM TEMED or (*D*) 12.5 mM APS/6.25 mM TEMED, showing differences in gel distribution based on initiator concentrations. (Scale bars, 10 mm.) (*E*) Representative H&E-stained image of the cardiac tissue at the apex of a MeHA High gel (labeled "G")-treated infarct 24 h postinjection, demonstrating integration with tissue. (Scale bar, 100 μm.)

of the hydrogel in the tissue was observed with hydrogels formed with a lower initiator concentration and slower gelation time than with hydrogels formed with a higher initiator concentration and faster gelation (Fig. 1 *C* and *D*). The high initiator concentration also led to a more rapid increase in viscosity, making the hydrogel more difficult to inject. Based on these findings, the 5.0 mM APS and 5.0 mM TEMED initiator combination was selected for all remaining studies. Importantly, gel distribution was not dependent on the MeHA formulation, as long as the initiator concentration was constant. When the hydrogel was injected in vivo and assessed 24 h post-MI (Fig. 1*E*), histological staining demonstrates a clear integration of the gel within the tissue and distribution throughout cell layers (Fig. 1*E*).

Furthermore, bulk hydrogels formed from these macromer/initiator combinations lost less than 25% of their mass after 20 wk in PBS at 37 °C [as measured using the uronic acid assay (27)], and there was no statistically significant difference in the overall percentage of hyaluronic acid release or profiles throughout degradation (Fig. 2*A*). A decrease in the modulus of bulk hydrogels, especially with MeHA High, is noted with time (Fig. S3). Cytotoxicity was evaluated through exposure of seeded human mesenchymal stem cells to sterilized bulk hydrogels (formed using the same initiation conditions) in a Transwell format for up to 3 d; no differences were observed with any of the gels compared with unexposed controls (Fig. S4).

Hydrogel Injection Impacts Mechanics of Cardiac Tissue. To confirm further that the differences in hydrogel mechanics were maintained upon injection into cardiac tissue, the mechanics of bulk hydrogels alone, explanted cardiac tissue alone, and hydrogel/tissue composites were assessed. Under compression, the modulus of untreated cardiac tissue was 5.8 ± 1.5 kPa, whereas the bulk hydrogels had moduli of 7.7 ± 1.0 kPa and 43.0 ± 12.3 kPa for MeHA Low and MeHA High, respectively. The modulus of the tissue/hydrogel composite was greater than explanted cardiac tissue alone for the MeHA High group but not for the MeHA Low group (Fig. 2*B*). Specifically, with the MeHA Low gel there was no statistical difference in the modulus between the cardiac tissue and the composite; however, there was a statistically significant increase in modulus with the MeHA High composite when compared with normal cardiac tissue. Similar trends were observed when the tissue/hydrogel composites underwent uniaxial tensile testing in the longitudinal direction (Fig. S5).

Hydrogel Injection Maintains Normal Tissue Thickness and Reduces Infarct Size Depending on Modification. Injection of the MeHA hydrogels 30 min after infarction (Fig. S6 shows a representative injection pattern) led to maintenance of tissue thickness compared with control infarct samples, as evident upon sacrifice at 8 wk (Fig. 3 *A*–*C*). The regional thickness from the apex to the base was quantified and demonstrated significant differences in tissue thickness for MeHA High and MeHA Low hydrogel injections in the apex (7.02 and 6.54 mm, respectively) and basilar infarct (7.15 and 6.96 mm, respectively) regions, compared with control infarct apex (2.13 mm) and basilar infarct (4.89 mm) regions (Fig. 3*D*).

This prevention of tissue thinning also is evident upon examination of the representative histological images in Fig. 4. Magnified images of samples with MeHA High (Fig. 4*D* and Fig. S7*D*) and MeHA Low (Fig. 4*E* and Fig. S7*E*) treatment show that the gels are present and maintain their integration with the tissue at 8 wk.

The length of abnormal motion in the anteroapical wall immediately after coronary occlusion and before injection was similar in all groups, indicating that the stimulus for remodeling (i.e., initial infarct size) was comparable among the three groups (Fig. 5*A*). However, the infarct area at the time of sacrifice was smaller with MeHA treatment (23.9% MeHA High, $P < 0.05$, and 26.4% MeHA Low) than in the control infarct (28.6%), indicating that the treatment groups experienced less infarct expansion during the 8-wk follow-up period (Fig. 5*A*). The nonstatstically

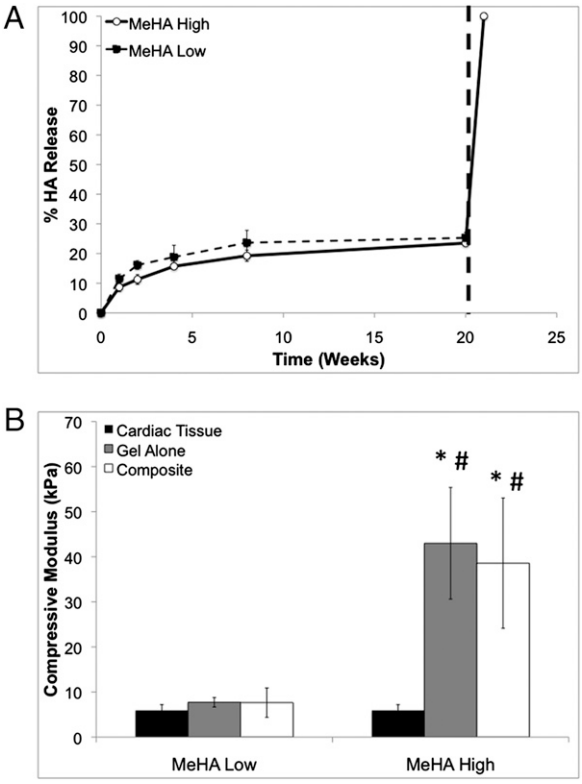

Fig. 2. Hydrogel degradation and compressive mechanics. (*A*) MeHA High (circle, solid line, $n = 3$) and MeHA Low (square, dotted line, $n = 3$) degradation with time. The percentage of hyaluronic acid release was quantified with the uronic acid (a by-product of hyaluronic acid degradation) assay. The vertical dashed line represents the addition of 100 U/mL exogenous hyaluronidase at 20 wk to initiate complete degradation. (*B*) Mechanical properties of cardiac tissue, MeHA hydrogel, and hydrogel/tissue composite. $n = 5$ per group. Data are presented as mean ± SD. $^{*}P < 0.05$ compared with cardiac tissue, $^{\#}P < 0.05$ compared with MeHA Low for the respective condition.

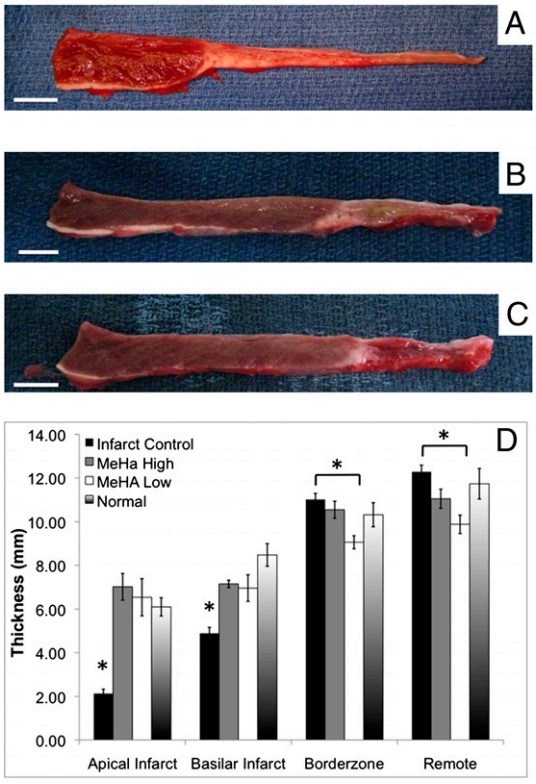

Fig. 3. Hydrogel treatment influences myocardial wall thickness. Representative samples of (*A*) control infarct ($n = 9$), (*B*) MeHA High treatment ($n = 6$), and (*C*) MeHA Low treatment ($n = 5$) 8 wk post-MI and hydrogel injection. (*D*) Quantified regional tissue thicknesses at 8 wk ($n = 5$ for Normal). Data are presented as mean ± SEM. $^{*}P < 0.05$ compared with all other groups in the same region. (Scale bar, 10 mm.)

significant trend toward smaller lengths of abnormal motion in the anteroapical wall motion abnormality in the MeHA High group lends support to this conclusion (Table S1).

Hydrogel Injection Attenuates LV Dilation and Improves Cardiac Function Depending on Hydrogel Mechanics. Real-time 3D echocardiography was used to assess the LV dimensions and cardiac function for each animal before and immediately after (i.e., baseline) infarction. The normalized end-diastolic volume (NEDV) and normalized end-systolic volume (NESV) increased for all groups after 2 wk, with the MeHA High treatment group tending to have the smallest changes in volume (Table S1). A similar trend was observed after 8 wk, with the MeHA High treatment group again demonstrating an improvement (i.e., lower) in NEDV (1.7; Fig. 5*B*) and NESV (1.9; Fig. 5*B*) compared with the infarct control (2.1 and 2.4, respectively) and the MeHA Low treatment group (2.1 and 2.5, respectively). This improvement was even more dramatic upon stress testing with dobutamine (2.5 and 5.0 $mg{\cdot}kg^{-1}min^{-1}$), which was conducted before sacrifice (Table S1).

The cardiac output was reduced for all groups at 2 and 8 wk following MI, although this difference was statistically different from the baseline only for the control infarct group (Fig. 5*C* and Table S1). A reduction in the ejection fraction (EF) at 2 and 8 wk also was observed for all groups relative to their respective baseline values (Fig. 5*C* and Table S1). Stress testing before sacrifice demonstrated a greater improvement in EF of the MeHA High treatment group (Table S1).

Discussion

The LV remodeling that occurs post-MI is a complex process, and increased understanding of this process, as well as of the impact of various treatment paradigms, is needed to develop valuable therapies to improve patient outcomes and welfare. LV remodeling evolves with time post-MI to involve myocardium more remote from the infarct in a process known as "borderzone expansion" (6, 11, 12, 15). The reduced wall thickness in the infarct region and a global change to a more spherical geometry correspond to increases in wall stress (6, 11, 12). These alterations increase the mechanical burden on the injured heart and

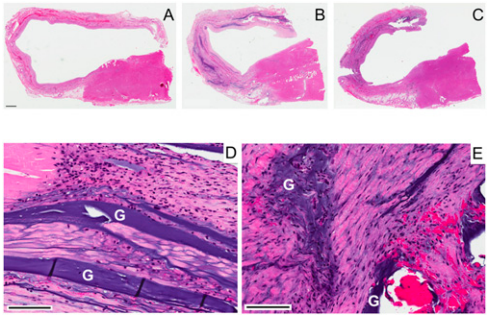

Fig. 4. Histological images at 8 wk post-MI and injection. Representative H&E-stained samples of (*A*) control infarct, (*B* and *D*) MeHA High, and (*C* and *E*) MeHA Low treatment in which the gel (labeled "G") stains purple. (Scale bar, 1 mm in *A*–*C*, 100 μm in *D* and *E*.)

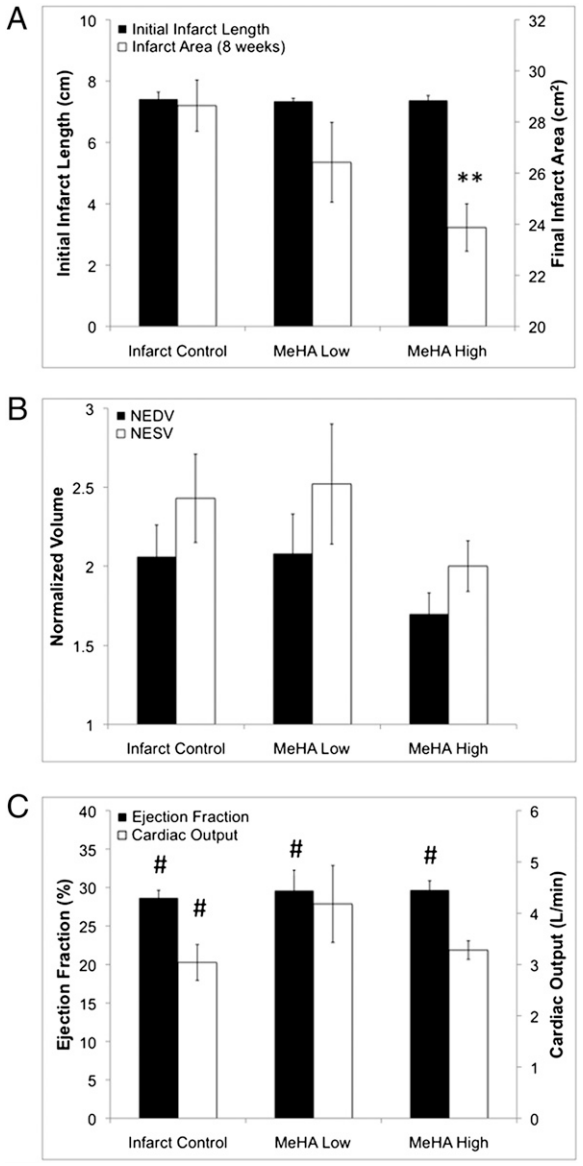

Fig. 5. Quantified infarct dimensions, in vivo volume, and functional metrics for control infarct ($n = 9$), MeHA High treatment ($n = 6$), and MeHA Low treatment ($n = 5$). (*A*) Initial infarct length and infarct area at 8 wk. (*B*) NEDV and NESV. (*C*) Cardiac output and EF. Data are presented as mean ± SEM. $^{*}P < 0.05$ versus control infarct; $^{\#}P < 0.05$ versus respective baseline value.

initiate maladaptive biological processes that act together to produce heart failure (11, 12). Although recent data have demonstrated that injectable materials can affect the post-MI LV remodeling (17–24, 26, 28), only a few groups (23, 25, 26) have evaluated the impact of acellular intramyocardial injections in large-animal models of MI (e.g., swine or ovine). Furthermore, the influence of specific material properties on the associated LV remodeling response has not been explored experimentally and is not well understood. This lack of information is caused in part by the difficulty in developing materials that can be used to investigate systematically the influence of one property (e.g., mechanics) without altering other potentially confounding parameters (e.g., mass loss).

In this study, we investigated hyaluronic acid hydrogels in which mechanical properties are modified through a simple alteration in the number of reactive methacrylate groups (i.e., MeHA Low versus MeHA High) on the MeHA macromer, a change that is made easily during synthesis. After crosslinking with the redox initiation system, the extent of modification leads to variations in the crosslinking density of the hydrogels, and these variations correlate with changes in bulk mechanical properties while maintaining the same concentration of the material. Changes in the initiator concentration (i.e., onset of gelation) led to variations in the distribution of the hydrogel within the myocardial tissue, another parameter that may be important in therapy development as well as in the mechanics of a specific MeHA formulation. However, the time for gelation did not depend on the extent of methacrylation. Notably, mass loss also did not differ between the two MeHA formulations. Although the hydrogels undergo a small amount of bulk hydrolytic degradation (because of ester bonds in the methacrylate group), and the compressive moduli of the hydrogels change moderately with time, they remain greater than (MeHA High) or similar to (MeHA Low) cardiac tissue even after 8 wk of in vitro degradation. Thus, this system allows investigation of the influence of hydrogel mechanics on the resulting therapeutic outcomes for treating MI, without variations in material amount, degradation, or tissue distribution to confound the findings.

Investigation of the mechanics of cardiac tissue before and after injection of the hydrogels revealed an increased modulus with hydrogel injection, dependent on the MeHA modification. A constant initiator system of 5.0 mM APS/5.0 mM TEMED was selected to maximize material distribution at each injection site. The injection process leads to a series of hydrogel pockets that distribute from the injection point, making it difficult to obtain uniform samples for composite material testing. Thus, compression was used to minimize non-uniformity of the samples, and it was possible to core the samples that appeared uniform. Similar trends were observed upon uniaxial tensile testing of tissue/hydrogel composites in the longitudinal direction. However, because of the thickness of the wall, samples were isolated from the midwall, leading to variability in fiber angle that further contributed to the observed variations. Histological evaluation of a hydrogel/tissue composite at 24 h postinjection in vivo demonstrated stable gel formation and integration of the gel within the tissue, and this stability still was observed even at 8 wk postinjection. Thus, the stability of the materials indicates that the primary difference between the two groups was the mechanical properties of the hydrogel. Furthermore, the cellular response to MeHA is very limited, with no evidence of increased macrophage or myofibroblast infiltration. The change in infarct expansion and functional properties appear to relate to the properties of the injectate rather than a biologic response to the material. A finite element simulation of the theoretical impact of injection of a material into the myocardium after MI illustrates the suspected potential of intramyocardial stiffening in reducing stress. Furthermore, stiffer materials were shown to bear more of the load in the remote and borderzone regions, resulting in a decrease in stresses within these regions (28). Moreover, using a closed-loop lumped-parameter model of the ovine cardiovascular system, we also have demonstrated that a reduction in compliance in the infarct area (i.e., infarct stiffening) should reduce dilation of the LV and improve EF (29). For this reason, specific formulations were investigated to form hydrogel/tissue composites that have similar (MeHA Low) and greater (MeHA High) moduli than native cardiac tissue. Hydrogels were injected 30 min postinfarction into 20 injection sites in the apex and borderzone region, and outcomes were assessed after 2 and 8 wk and by dobutamine stress evaluation immediately before sacrifice. To limit animal mortality, we chose to intervene at 30 min postinfarction; this timing probably is faster than could be achieved clinically because the average time from onset of symptoms to hospital presentation averages 2–6 h (30, 31). However, recent reports also have demonstrated attenuation of LV remodeling with polymer injection several weeks after infarct (32, 33). Future work will evaluate the impact of MeHA treatment time and

infarct reperfusion status on LV remodeling. This MI model involves a permanent occlusion, which generally is associated with a more profound remodeling stimulus (34, 35) than in reperfused infarct models that have been used to evaluate the impact of other injectable materials with reperfusion (17, 25, 36).

Unfortunately, little is known regarding changes in infarct material properties with time and reperfusion status, factors that may affect the optimal properties of the injectable material. It was our intent to use our MeHA system to isolate one variable (e.g., injected hydrogel mechanics) to evaluate systematically the resulting impact on infarct expansion and remodeling. This work contributes to the development of injectable materials for therapy and provides further insight into the pathobiology that occurs post-MI. Future work in our laboratory will involve further examination of the change of infarct material properties (e.g., tissue mechanics) with time and hydrogel (e.g., nondegradable versus degradable) treatment.

A statistical difference in wall thickness in the apex and basilar infarct regions was evident for both MeHA treatment groups relative to the infarct control. Importantly, these groups had wall thicknesses similar to noninfarct controls. This drastic difference in tissue thickness is further evident upon examination of the histological images. Although infarct thicknesses increased in both treatment groups relative to control, significantly less infarct expansion and reduced LV remodeling was seen only with the MeHA High formulation. This result suggests that the properties of the injected material (i.e., increased stiffness) may be of greater importance in stress reduction than infarct stiffening alone.

The global LV geometry was evaluated using real-time 3D echocardiography. At the 2- and 8-wk time points, an increase in NEDV and NESV for all groups was observed. However, at both time points the MeHA High treatment group had smaller changes in volume than seen in the control infarct and MeHA Low treatment groups. Furthermore, the differences in both NEDV and NESV from the 2-wk to the 8-wk time point are lowest for the MeHA High treatment group. The improvement in LV volume in the MeHA High treatment group is even clearer upon the stress testing that was completed before sacrifice at 8 wk. These observations are important, because increased end-systolic volume is indicative of adverse effects post-MI (37). LV function was assessed by monitoring cardiac output and EF throughout the study. The control infarct group had statistically different values at the 2-wk and 8-wk follow-ups, whereas both the MeHA treatment groups did not. As expected, a decrease in EF was observed for all treatment groups at the 2- and 8-wk follow-ups. Again, the MeHA High treatment group tended to have improved EF, which was more dramatic upon stress testing.

The goal of this study was to investigate any salutary effects associated with differences in the mechanics of the injectable hydrogels developed to limit infarct expansion and to suppress the LV remodeling response that occurs post-MI. Our findings clearly indicate that the group treated with higher modulus hydrogel demonstrated less infarct expansion and reduced LV dilation, as well as improved function when compared with our lower modulus hydrogel and infarct control groups. In agreement with the simulations described by Wall et al. (28), we believe that the higher modulus MeHA hydrogel is better able to stabilize the myocardium and reduce wall stresses than the lower modulus MeHA hydrogel. Because the modulus of the tissue/ MeHA Low composite group is similar to that of the excised cardiac tissue, it is likely that these values are closer to the passive material properties of the myocardium during diastole, whereas the modulus of the tissue/MeHA High composite probably is closer to passive myocardial material properties at end-systole. Because the increase in wall stress during systole probably drives the maladaptive remodeling process, the tissue treated with MeHA High may be more capable of normalizing myocardial stress distribution than tissue treated with MeHA Low.

This study evaluates the impact in vivo of the properties of an injectable material on the post-MI LV remodeling response and provides fundamental information that can be used in developing hydrogels for treatment of LV remodeling. However, further work to determine the impact of hydrogel degradation (i.e., changes in material properties with time) is needed. Moreover, the timing of therapy (e.g., acute versus chronic), mode of delivery (e.g., via a catheter), and possible encapsulation of cells or drugs should be investigated to develop an optimal system for clinical use in the treatment of MI.

Materials and Methods

The animals used in this work received care in compliance with the protocols approved by the Institutional Animal Care and Use Committee at the University of Pennsylvania in accordance with the guidelines for humane care (National Institutes of Health Publication 85-23, revised 1996).

Macromer Synthesis and Characterization. MeHA was synthesized as previously described (38). Briefly, sodium hyaluronate (74 kDa; Lifecore) was dissolved at 1% by weight in deionized water and reacted with methacrylic anhydride (Sigma) at pH 8.0 on ice for 24 h with varied amounts of methacrylic anhydride to influence the final macromer methacrylation. The macromer was purified via dialysis (molecular weight cutoff, 6–8 kDa) against deionized water for 72 h and lyophilized. ^{1}H NMR (Bruker) was used to determine the % methacrylation.

In general, MeHA (4% by weight) was dissolved in PBS with various concentrations of APS (5.0 or 12.5 mM; Sigma) and TEMED (5.0 or 6.25 mM; Sigma). Gelation onset (n = 3) was quantified by monitoring the storage (G′) and loss (G″) moduli with time using an AR2000ex Rheometer (TA Instruments) at 37 °C under 1% strain and 1 Hz in a cone and plate geometry (1°, 20-mm diameter). MeHA/APS and MeHA/TEMED solutions were loaded into different barrels of a dual-barrel syringe and crosslinked by expulsion and mixing from the syringe. Compression testing was completed on hydrated samples (5-mm diameter; n = 3) using a Dynamic Mechanical Analyzer (Q800; TA Instruments) at a strain rate of 10% min^{-1}. Degradation (n = 3 per time point) in PBS at 37 °C was monitored using a uronic acid assay (27), and 100 units of exogenous hyaluronidase per mL PBS was added at 20 wk for complete degradation of the hydrogels. (Methods of cytotoxicity evaluation are given in *SI Materials and Methods*.) For in vivo assessment, the lyophilized form of MeHA was sterilized by exposure to germicidal UV light for 1 h and subsequently dissolved in sterile PBS. APS and TEMED solutions were sterile filtered before use in vivo.

Explanted Tissue. The delivery and penetration of the injected hydrogel into normal (not infarcted) myocardial tissue was investigated using explanted ovine myocardial tissue from the LV apex (i.e., the intended infarct region). For visualization purposes, 125 μM methacryloxethyl thiocarbamoyl rhodamine B was added. This dye is macroscopically visible and crosslinks into the hydrogel. To confirm gelation within the tissue, 0.3 mL of the macromer/initiator solution with dye was injected into the LV apex. After 30 min, biopsy punches were used to remove 5-mm-diameter disks of tissue or tissue containing hydrogel composite for compression testing (n = 5 per group from multiple samples from two hearts), as above. (Methods of uniaxial tensile testing are detailed in *SI Materials and Methods*.)

Infarction Model and in Vivo Assessment. A clinically relevant ovine model of infarction and LV remodeling was used to assess the impact of the injected hydrogels (23). Twenty-one adult male Dorset sheep (35–40 kg) were anesthetized. The arterial, ventricular, and pulmonary artery pressures and electrocardiogram were monitored continuously throughout the procedure. A left thoracotomy was performed to expose the heart. Baseline echocardiographic and hemodynamic data were obtained. Infarction was induced via ligation of the left anterior descending and the second diagonal coronary artery to create an infarct the basal extent of which was 40% of the distance from the apex to the base of the heart. This procedure previously demonstrated the creation of a reproducible, moderately sized infarct involving ~20% of the LV mass at the anteroapex (39).

Animals were assigned to the following three cohorts: infarct control (n = 9), MeHA High (n = 7), and MeHA Low (n = 5). Historical data of normal (noninfarct) tissue thickness was used for comparisons. Cohorts receiving MeHA treatment received 20 injections of 0.3-mL macromer/initiator solution at 3 min postmixing immediately following the echocardiograph at

30 min following infarction. The injection sites were distributed uniformly within the ischemic territory and located at a depth of ≈2 mm into the midwall of the myocardium. Echocardiographic data were collected and analyzed as previously described (23). (Further details on echocardiographic analysis are given in *SI Materials and Methods*.)

Echocardiographic and hemodynamic data were collected again at 2 and 8 wk postinfarct. Animals also underwent dobutamine (2.5 and 5.0 mg kg^{-1} min^{-1}) stress echocardiographic testing at 8 wk. After these evaluations, animals were killed, the hearts were harvested, and the infarct thickness was measured with a digital micrometer. Samples also were collected and fixed for histological analysis using H&E staining and Mason's trichrome staining. One MeHA High treatment subject was killed at 24 h postinjection and processed for histology to evaluate gel distribution in vivo.

Statistical Analysis. Data are presented as mean ± SD or mean ± SEM as indicated in the figure legends. For hydrogel characterization experiments, differences between groups were assessed using the Student's *t* test. Changes in tissue dimensions and echocardiograph and LV function readings were assessed using a one-way ANOVA with Tukey's post hoc evaluation. Echocardiographic and LV function readings were compared using a paired *t* test for comparisons with baseline values for a respective group. For all comparisons, $P < 0.05$ was considered statistically significant.

ACKNOWLEDGMENTS. This work was supported by an American Heart Association Predoctoral Fellowship and an Ashton Foundation Fellowship (to J.L.I.), a Wallace H. Coulter Early Career Investigator Award (to J.A.B.), National Institutes of Health Grants HL63954 (to R.C.G.), HL73021 (to J.H.G.), and HL76560 (to J.H.G.), and individual Established Investigator Awards from the American Heart Association (to J.H.G. and R.C.G.).

1. Gheorghiade M, Bonow RO (1998) Chronic heart failure in the United States: A manifestation of coronary artery disease. *Circulation* 97:282–289.
2. Eaton LW, Weiss JL, Bulkley BH, Garrison JB, Weisfeldt ML (1979) Regional cardiac dilatation after acute myocardial infarction: Recognition by two-dimensional echocardiography. *N Engl J Med* 300:57–62.
3. Erlebacher JA, Weiss JL, Weisfeldt ML, Bulkley BH (1984) Early dilation of the infarcted segment in acute transmural myocardial infarction: Role of infarct expansion in acute left ventricular enlargement. *J Am Coll Cardiol* 4:201–208.
4. Weisman HF, Healy B (1987) Myocardial infarct expansion, infarct extension, and reinfarction: Pathophysiologic concepts. *Prog Cardiovasc Dis* 30:73–110.
5. Epstein FH, et al. (2002) MR tagging early after myocardial infarction in mice demonstrates contractile dysfunction in adjacent and remote regions. *Magn Reson Med* 48:399–403.
6. Jackson BM, et al. (2002) Extension of borderzone myocardium in postinfarction dilated cardiomyopathy. *J Am Coll Cardiol* 40:1160–1167, discussion 1168–1171.
7. Jackson BM, et al. (2003) Border zone geometry increases wall stress after myocardial infarction: Contrast echocardiographic assessment. *Am J Physiol Heart Circ Physiol* 284:H475–H479.
8. Kramer CM, et al. (1993) Regional differences in function within noninfarcted myocardium during left ventricular remodeling. *Circulation* 88:1279–1288.
9. Lima JAC, et al. (1985) Impaired thickening of nonischemic myocardium during acute regional ischemia in the dog. *Circulation* 71:1048–1059.
10. Pilla JJ, et al. (2005) Early postinfarction ventricular restraint improves borderzone wall thickening dynamics during remodeling. *Ann Thorac Surg* 80:2257–2262.
11. Gorman RC, Jackson BM, Gorman JH (2004) The potential role of ventricular compressive therapy. *Surg Clin North Am* 84:45–59.
12. Mann DL (1999) Mechanisms and models in heart failure: A combinatorial approach. *Circulation* 100:999–1008.
13. Blom AS, et al. (2005) Infarct size reduction and attenuation of global left ventricular remodeling with the CorCap cardiac support device following acute myocardial infarction in sheep. *Heart Fail Rev* 10:125–139.
14. Enomoto Y, et al. (2005) Early ventricular restraint after myocardial infarction: Extent of the wrap determines the outcome of remodeling. *Ann Thorac Surg* 79:881–887, discussion 881–887.
15. Kelley ST, et al. (1999) Restraining infarct expansion preserves left ventricular geometry and function after acute anteroapical infarction. *Circulation* 99:135–142.
16. Moainie SL, et al. (2002) Infarct restraint attenuates remodeling and reduces chronic ischemic mitral regurgitation after postero-lateral infarction. *Ann Thorac Surg* 74: 444–449, discussion 449.
17. Christman KL, Fok HH, Sievers RE, Fang QH, Lee RJ (2004) Fibrin glue alone and skeletal myoblasts in a fibrin scaffold preserve cardiac function after myocardial infarction. *Tissue Eng* 10:403–409.
18. Dai WD, Wold LE, Dow JS, Kloner RA (2005) Thickening of the infarcted wall by collagen injection improves left ventricular function in rats: A novel approach to preserve cardiac function after myocardial infarction. *J Am Coll Cardiol* 46:714–719.
19. Davis ME, et al. (2006) Local myocardial insulin-like growth factor 1 (IGF-1) delivery with biotinylated peptide nanofibers improves cell therapy for myocardial infarction. *Proc Natl Acad Sci USA* 103:8155–8160.
20. Dobner S, Bezuidenhout D, Govender P, Zilla P, Davies N (2009) A synthetic non-degradable polyethylene glycol hydrogel retards adverse post-infarct left ventricular remodeling. *J Card Fail* 15:629–636.
21. Fujimoto KL, et al. (2009) Synthesis, characterization and therapeutic efficacy of a biodegradable, thermoresponsive hydrogel designed for application in chronic infarcted myocardium. *Biomaterials* 30:4357–4368.
22. Kofidis T, et al. (2005) Novel injectable bioartificial tissue facilitates targeted, less invasive, large-scale tissue restoration on the beating heart after myocardial injury. *Circulation* 112(9, Suppl):I173–I177.
23. Ryan LP, et al. (2009) Dermal filler injection: A novel approach for limiting infarct expansion. *Ann Thorac Surg* 87:148–155.
24. Singelyn JM, et al. (2009) Naturally derived myocardial matrix as an injectable scaffold for cardiac tissue engineering. *Biomaterials* 30:5409–5416.
25. Leor J, et al. (2009) Intracoronary injection of in situ forming alginate hydrogel reverses left ventricular remodeling after myocardial infarction in swine. *J Am Coll Cardiol* 54: 1014–1023.
26. Mukherjee R, et al. (2008) Targeted myocardial microinjections of a biocomposite material reduces infarct expansion in pigs. *Ann Thorac Surg* 86:1268–1276.
27. Bitter T, Muir HM (1962) A modified uronic acid carbazole reaction. *Anal Biochem* 4: 330–334.
28. Wall ST, Walker JC, Healy KE, Ratcliffe MB, Guccione JM (2006) Theoretical impact of the injection of material into the myocardium: A finite element model simulation. *Circulation* 114:2627–2635.
29. Pilla JJ, Gorman JH, 3rd, Gorman RC (2009) Theoretic impact of infarct compliance on left ventricular function. *Ann Thorac Surg* 87:803–810.
30. Jneid H, et al.; Get With the Guidelines Steering Committee and Investigators (2008) Impact of time of presentation on the care and outcomes of acute myocardial infarction. *Circulation* 117:2502–2509.
31. Miura T, Miki T (2008) Limitation of myocardial infarct size in the clinical setting: Current status and challenges in translating animal experiments into clinical therapy. *Basic Res Cardiol* 103:501–513.
32. Landa N, et al. (2008) Effect of injectable alginate implant on cardiac remodeling and function after recent and old infarcts in rat. *Circulation* 117:1388–1396.
33. Yu JS, et al. (2009) Restoration of left ventricular geometry and improvement of left ventricular function in a rodent model of chronic ischemic cardiomyopathy. *J Thorac Cardiovasc Surg* 137:180–187.
34. Kloner RA, Hwang H (2008) New insights into the open artery hypothesis. *Circ Res* 103:1–3.
35. Hochman JS, Choo H (1987) Limitation of myocardial infarct expansion by reperfusion independent of myocardial salvage. *Circulation* 75:299–306.
36. Christman KL, et al. (2004) Injectable fibrin scaffold improves cell transplant survival, reduces infarct expansion, and induces neovasculature formation in ischemic myocardium. *J Am Coll Cardiol* 44:654–660.
37. Opie LH (2005) Ventricular function. *Essential Cardiology: Principles and Practice*, ed Rosendorff C (Humana, Totowa, NJ), 2nd Ed, pp 37–54.
38. Burdick JA, Chung C, Jia XQ, Randolph MA, Langer R (2005) Controlled degradation and mechanical behavior of photopolymerized hyaluronic acid networks. *Biomacromolecules* 6: 386–391.
39. Markovitz LJ, et al. (1989) Large animal model of left ventricular aneurysm. *Ann Thorac Surg* 48:838–845.